



LAWRENCE  
LIVERMORE  
NATIONAL  
LABORATORY

# Barometric Calorimeter Experiments with C4 Charges

A. L. Kuhl, J. Tringe, K. Vandersall, W. M. Howard

January 5, 2012

34th International Combustion Symposium  
Warsaw, Poland  
July 29, 2012 through August 3, 2012

## **Disclaimer**

---

This document was prepared as an account of work sponsored by an agency of the United States government. Neither the United States government nor Lawrence Livermore National Security, LLC, nor any of their employees makes any warranty, expressed or implied, or assumes any legal liability or responsibility for the accuracy, completeness, or usefulness of any information, apparatus, product, or process disclosed, or represents that its use would not infringe privately owned rights. Reference herein to any specific commercial product, process, or service by trade name, trademark, manufacturer, or otherwise does not necessarily constitute or imply its endorsement, recommendation, or favoring by the United States government or Lawrence Livermore National Security, LLC. The views and opinions of authors expressed herein do not necessarily state or reflect those of the United States government or Lawrence Livermore National Security, LLC, and shall not be used for advertising or product endorsement purposes.

## Barometric Calorimeter Experiments with C4 Charges

A. L. Kuhl, J. Tringe, K. Vandersall, W. M. Howard

Lawrence Livermore National Laboratory, P.O. Box 808, Livermore, CA 94551 USA

---

### ABSTRACT

Experiments were conducted in our 506-liter barometric calorimeter, to characterize the reflected blast wave environment from C-4 explosions. Charges were constructed as a C4 hemi-sphere and boosted by a LX-10 hemi-sphere. The charge was placed in the center of the calorimeter and initiated by an SE-1 detonator. The blast wave was measured by Kistler piezo-electric pressure gauges, located at 8 radii on the chamber lid. Six experiments were conducted: three in air, and three in nitrogen (to eliminate combustion effects). Blast waves in air arrived earlier than those in nitrogen. Reflected pressure impulses were 7% larger for the air experiments than for those in nitrogen—thereby quantifying the effects that combustion has on C4 blast waves. Late-time chamber pressures were measured with a Kulite piezo-resistive gauge. Measured chamber pressures were 2 times larger for the air experiments than for those in nitrogen—thereby quantifying the effects that C4-air combustion has on late-time pressures. Results were fit with analytic functions to establish scaling laws that show how the reflected blast wave pressures and impulses depend on charge mass and height of burst (HOB).

*Keywords:* C4 Detonation Products, Turbulent Combustion, Barometric Calorimeter

---

### 1. Introduction

In traditional calorimeter experiments, the temperature rise of a water bath is used to evaluate caloric value of an explosion. For example, Ornellas [1] measured the heat of detonation for 46 explosives in a 5.3-liter spherical bomb calorimeter. In one set of experiments, 25-g TNT charges were detonated in vacuum conditions; explosion energy of 1,093 cal/g was measured, which is in good agreement with the *heat of detonation* 1,133 cal/g for TNT as predicted by the CHEETAH code [2]. In companion experiments, 25-g TNT charges were detonated in an oxygen atmosphere pressurized to 2.46 bars; explosion energy of 3,575 cal/g was measured, which is in good agreement with the *heat of combustion* of 3,594 cal/g for TNT-air [2]. While such experiments can confirm the heats of detonation

and combustion and the composition of explosion products, they give no information on the time evolution of energy (e.g, afterburning with air).

To overcome this, we have developed a *barometric calorimeter technique*—whereby pressure histories are used to characterize the gasdynamic consequences of exothermic process. In particular, pressure measurements can be used both to measure the blast wave created by detonation of the charge and to evaluate the caloric value of an explosion. By performing experiments in air and nitrogen ( $N_2$ ) atmospheres, one can separate out blast wave effects resulting from the detonation of the charge (in  $N_2$ ) from afterburning effects associated with the turbulent mixing and combustion of detonation products ( $DP$ ) with air. To this end, six different barometric calorimeters were constructed [3], with volumes ranging from 6.6 to 40 liters with  $L/D$  ratios of 1, 3.9, 4.7 and 12.5. These were used to evaluate combustion effects in confined explosions [4] of 1.5 g charges of TNT and Aluminum powder. Numerical simulations of the turbulent combustion occurring in the experiments were performed with an AMR combustion code [5,6,7,8]. A theory that describes locus of combustion states in thermodynamic state space has been developed [9].

## 2. Barometric Calorimeter

To study combustion effects in explosions from other (non-ideal) charges, which have much larger reaction-zone thicknesses, a larger scale calorimeter is needed. To this end, we designed and built a 506-liter calorimeter. The calorimeter was a right circular cylinder ( $d = h = 86 \text{ cm}$ ) of volume 506 liters, with 5 cm thick steel walls, floor and lid (Fig. 1). It was designed to withstand static pressures of 12 bars, corresponding to the detonation of 100-g TNT charges, and the combustion of its detonation products gases with air. The principal diagnostics were piezoelectric pressure gauges (Kistler 603B); 8 gauges were flush-mounted on the lid of the container at different radii ( $GR = 0, 5, 10, 15, 20, 25$  and

30.5 cm) and recorded on a Yokogawa scope (DL-750) at a sampling rate of 0.1  $\mu$ s. In addition, a piezoresistive pressure gauge (Kulite HEM 375) was located at  $GR = 20$  cm; this was used to measure the late-time chamber pressure. Feasibility tests were conducted with 50-g charges and simulated with the ALE3D code; results were reported at the 14<sup>th</sup> Int. Detonation Symposium [10].

### 3. Charge Configuration

The charge configuration consisted of the following assembly (Fig. 2). A hemi-spherical shell (6 cm diameter,  $\sim 1$  mm wall thickness) of ABS plastic was formed on a rapid prototyping machine. This hemi-sphere was filled with  $m$  grams of C4. Another hemi-spherical shell (3 cm diameter,  $\sim 1$  mm wall thickness) of ABS plastic was filled with LX-10, which served as a booster. The booster shell was pressed into the C4 for good contact. This assembly was attached to a Lexan cylinder ( $d = 6$  cm,  $l = 5$  cm), which served as a mounting stand (Fig. 2). The booster was ignited with an SE-1 detonator [11] (PETN/Tetryl,  $d = 0.85$  cm), which was flush mounted at the Lexan surface. This assembly was mounted in the center of the calorimeter (with C4 hemisphere base located at the mid-plane of the chamber). This hemi-spherical charge configuration was selected because: (i) it had a high probability of causing the main charge to detonate; (ii) it created a hemi-spherical blast wave in the upper half plane of the chamber, which well models a spherical blast wave for the first blast wave reflection; (iii) the charge configuration could accommodate liquid or powder reactive materials (which can react but do not detonate); (iv) it could be fielded without a charge development program. In future tests, we plan to use a spherical charge configuration.

### 4. Experiments

Six experiments were performed: two tests with an air atmosphere in the chamber (tests #1 and #3), and two tests with a nitrogen atmosphere (tests #2 and #4) to suppress any combustion effects. In

addition, experiments with a bare charge (i.e. with the outer ABS plastic shell removed) were performed in air (test #5) and nitrogen (test #6) to determine whether the plastic shell influenced the reflected blast wave pressure field.

#### 4.1 Pressure histories

Pressure histories of the reflected blast wave from the hemi-spherical C4 detonated in air and nitrogen are compared in Figs. 3-9. Times are scaled by the characteristic time of the blast wave:  $t_0$  (see the Appendix for the scaling relations used to analyze the data). One can notice that the reflected blast wave arrived slightly sooner for tests in air than in nitrogen, and had a slightly higher peak pressure. This trend is systematic at all ground ranges. We offer this as evidence of additional energy release in the blast wave caused by combustion of detonation products gases with air.

#### 4.2 Positive-phase impulses

The positive-phase impulse of the reflected blast wave is defined as:

$$I_+ = \int_0^{t_+} \Delta p dt \quad (1)$$

where  $t_+$  denotes the positive phase (i.e., when the over-pressure history turns negative). Examination of Figs. 3-9 indicates that  $t_+ / t_0 = 0.062$  for these experiments. The positive-phase impulses were calculated from the pressure histories in Figs. 3-9; results were tabulated and scaled according to the relations in the Appendix. The non-dimensional positive-phase impulse is plotted as a function of ground range (GR), scaled by the characteristic length scale of the blast wave:  $r_0$  in Fig. 10. One can see that reflected blast wave impulse is slightly greater for tests in air than in nitrogen. This trend is systematic at all ground ranges, and is reflected in the curve fits 1 and 2 (air and  $N_2$ , respectively):

$$I_+(GR)_{air} = 0.924 - 3.7 * GR / r_0 \quad (2)$$

$$I_+(GR)_{N_2} = 0.859 - 3.7 * GR / r_0 \quad (3)$$

These curve fits indicate that the positive phase impulse is about 7% greater for tests in air, due to combustion of the *DP* products gases with air. Large variations of the impulse are evident at  $GR = 0$ ; this is due to jetting effects induced on axis. The SE-1 detonator acted as an area ignition source ( $d = 0.85$  cm) rather than a point source, causing stronger ignition along the axis thereby leading to jetting effects reflected in the pressures and impulses at  $GR = 0$ . Nevertheless, these experiments are able to quantify the extend of afterburning effects in C4 explosions; during the first positive phase, such effects are about 7% in impulse (under conditions studied).

#### 4.3 Chamber pressures

Kulite gauges measure overpressure:  $\Delta p \equiv p(t) - p_0$ , i.e., pressure enhancement about the initial atmospheric pressure in the chamber:  $p_0$ . Kulite gauges are designed for making pressure measurements for long durations<sup>1</sup>. Pressure histories measured by the Kulite gauge were integrated in time for tests #1-6. Impulses were fit with a linear function of time

$$I(t) \equiv a + \Delta p_c \cdot t \quad (4)$$

To accurately capture late-time pressures, the impulses were fit over the time domain:  $0.16 < t/t_0 < 3$ . Results are listed in Table 1. The slope of these curves represents the quasi-static chamber pressure  $\Delta p_c$ . Chamber pressures for C4 explosions in nitrogen agree with thermodynamic predictions (4.18 bars). Chamber pressures for C4 explosions in air are  $\sim 20\%$  higher than thermodynamic predictions (8.2 bars), due to the combustion of other materials (e.g., Lexan pedestal) in the chamber. Such effects will be eliminated in future tests by removing all combustibles from the chamber.

---

<sup>1</sup> Being based on piezo-resistive rather than piezo-electric principles, they do not suffer from late-time drift due charge bleed-off inherent in all piezo-electric gauges

## 5. Numerical simulations

To help in interpretation of the experiments, numerical simulations of the C4 charge explosion in a nitrogen atmosphere<sup>2</sup> were performed with the ALE3D code. A fine-zoned grid (mesh size of 160  $\mu\text{m}$ ) was used. Details of the charge assembly (Fig. 1a) were used to initialize the mesh. The PETN/Tetryl was initiated at a point, resulting in a propagating detonation, which was modeled with a programmed-burn model based on measured detonation velocities. This SE-1 detonation ignited the LX-10 booster, which then ignited the C4 charge; ignition and growth models were used to propagate those detonations. Jetting effects were evident along the axis, due to the finite-size effects of the initiation system.

Pressure histories were recorded along the reflecting plane at the same locations as the pressure gauges. Pressure histories from the numerical simulation were similar to the pressure histories measured in the nitrogen experiments; to conserve space, these will be made available in Supplemental Material. Instead, we compare the computed positive-phase impulses with data in Fig. 11. One can see that the computed points help to explain some of the wavy structure seen in the data versus ground range.

Peak pressures from the numerical simulation are compared with measured data in Fig. 12; in general, one can see that measured and computed peaks are in good agreement—except near the axis ( $GR = 0$ ). Peak pressures along the reflecting surface follow the linear relation (curve fit 3):

$$\Delta p_s / p_a = 168 - 750 * GR / r_0 \quad (5)$$

To sum up, Figs. 11 and 12 show that if one carefully models the initial charge configuration, and if one uses a proper specification of thermodynamic states of nitrogen (based on Cheetah code calculations), and if one uses enough grid resolution, then the ALE3D code can predict non-reactive blast wave environments from detonating charges such as C4 (i.e. it has captured all relevant physics).

---

<sup>2</sup> the nitrogen case was chosen because we do not have a combustion model of afterburning in the current version of the code.

The locus of thermodynamic states of reacting C4 blast waves is specified in the Le Chatelier diagram shown in Fig. 13. This figure includes loci for:

- *Fuel-F* (C4 detonation products states along the frozen isentrope passing through the CJ point)
- *Air-A* (isobar,  $p = 1$  atm)
- *Reactants-R* ( $F+A$  at a stoichiometric ratio of  $\sigma_s = A / F = 2.1$ )
- *Combustion Products-CP* (equilibrium products at a stoichiometry of  $\sigma_s$ )

In this formulation, combustion occurs at constant pressure and energy—so there is no addition of the “Heat of Combustion” to the system. At the beginning of the time step, one uses the frozen reactants curve, *R*, while at the end of the time step, one uses the equilibrium products curve, *CP*. Therefore, according to this formulation, the energy of the system is constant—a *system invariant*.

This combustion model has been implemented in our AMR code; numerical simulations of TNT combustion in barometric calorimeters were presented at the 33<sup>rd</sup> *Combustion Symposium* [5]. Figure 14 provides a visualization of the temperature field of an unconfined TNT combustion cloud in air [6]. Peak temperatures reach 2,900 K, corresponding to the adiabatic flame temperature of stoichiometric TNT-air mixtures. The rate of combustion is controlled by the turbulent mixing rate; by using adaptive mesh refinement, we are able to capture the energy-bearing scales of the turbulence [6]—and therefore compute accurate burning rates.

The above-mentioned AMR combustion code was used to simulate the C4 combustion in the barometric calorimeter experiments. Evolution of the C4 mass-fraction consumed by combustion with air is depicted in Fig. 15. One can see that the burning rate is slower at the beginning, corresponding to the induction time needed for transition to fully-developed turbulent flow. After that, the computed points are fit with a *life function* [12] (curve fit 4):

$$\mu(t) = 81.1 * [1 - 1.55e^{-14.8*t/t_0}] \quad (6)$$

By the end of the simulation, more than 70% of the C4 detonation products have been consumed; the fit indicates a fuel consumption of 81% at  $t = \infty$ .

## 6. Discussion

For practical applications, one must establish how these results scale to other situations. Here we follow the seminal scaling arguments of Brode [13]. For blast waves, two key parameters are important: the shock overpressure as a function of radius:  $\Delta p_s(r)$ , and the positive phase impulse  $I_+(HOB)$  as function of height of burst:  $HOB$ . These functions are displayed in non-dimensional form in Figs. 17 and 18 for C4 charges, and fit by the following:

$$\Delta p_s / p_a = -5.5 + 1.31 * (r / r_0)^{-5/3} \quad (7)$$

$$I_+ / p_a t_0 = 110 * (HOB / r_0)^{-7/3} \quad (8)$$

According to Nurik and Martin [14], the maximum displacement:  $\delta$  of thin metal plates (of thickness  $h$ ) is linearly proportional to the blast impulse:

$$\delta / h = C * I_+ \quad (9)$$

where C depends on the plate geometry and material properties. Combining eqs. (8) and (9), one finds how the maximum plate displacement depends of the charge mass  $m$  and standoff distance:  $HOB$ .

For sealed chambers, combustion effects become important. According to [9], the evolution of the chamber pressure obeys the following relation:

$$p_c(t) = p_R + \mu(t)[p_P - p_R] \quad (10)$$

where  $p_R$  and  $p_P$  denote the chamber pressure for frozen reactants (related to the Heat of Detonation) and equilibrium products (related to the Heat of Combustion), respectively. These may be evaluated by a constant-volume-explosion (CVE) model using the Cheetah code [2]. For C4 in the current barometric calorimeter, one finds  $p_R = 4.2 \text{ bars}$  and  $p_P = 8.2 \text{ bars}$ , so combustion increases the chamber pressure by about a factor of 2. This pressure enhancement evolves in time according to the life function  $\mu(t)$ , as specified eq. (6) for the current circumstances.

## 7. Conclusions

These experiments prove that the barometric calorimeter technique can both measure and quantify the effects that combustion has on reflected blast wave pressures and impulses (at early times), and on chamber pressures (at late times). This technique should be used to characterize combustion effects for other reactive materials.

## Acknowledgements

This work performed under the auspices of the U.S. Department of Energy by Lawrence Livermore National Laboratory under Contract DE-AC52-07NA27344. This work was funded by the Department of Homeland Security S&T under the contract number HSHQPM-10-X-00070. Their support is greatly appreciated.

## Appendix A

Scaling depends on atmospheric conditions and charge mass  $m$  [13]. Here we assumed the following values:  $p_a = 0.9918 \text{ bars}$ ,  $\rho_a = 1.204 \text{ mg/cc}$ ,  $T_a = 68F = 20C = 293K$ , and  $a_a = 339.597 \text{ m/s}$ , which correspond to the laboratory conditions at LLNL (altitude 180 meters above sea level). According to Sedov [15] and Brode [13] one can define a characteristic scale:  $r_0$  for spherical HE explosions as:

$$r_0 = [m * \Delta H_{ME} / p_a]^{1/3} \quad (A1)$$

It depends of the charge mass:  $m$ , the mechanical-energy component of the Heat of Detonation:  $\Delta H_{ME}$  and the atmospheric pressure  $p_a$ . In the present experiments with hemi-spherical charges, one actually needs to use  $2m$  in the above relation (corresponding to  $1m$  of energy in the upper hemispherical blast wave and  $1m$  of energy in the lower hemispherical blast wave). One can also define a corresponding characteristic time scale:  $t_0$  as:

$$t_0 = r_0 / a_a \quad (A2)$$

Characteristic scales have been evaluated for hemi-spherical C4 explosions for various charge masses; results are given in Table A1.

Table A1. Characteristic length and time scales for hemi-spherical C4 explosions\*

$m$ (g)	$r_0$ (cm)	$t_0$ (ms)
1	47.206	1.3902
10	101.70	2.9947
100	219.11	6.452
1,000	472.1	13.90

\* assumes  $2m$  in eq. (A1);  $\Delta H_{ME} = 1,248 \text{ cal / g}$  for C4 detonation

## References

- [1] Ornellas, D. L., *Calorimetric Determination of the Heat and Products of Detonation for Explosives: October 1961 to April 1982*, LLNL Report No. UCRL-52821, 1982, pp. 1-80.
- [2] Fried, L. E., *CHEETAH 1.22 User's Manual*, LLNL Report No. UCRL-MA-117541, 1995, 187 pp.
- [3] A. L. Kuhl, H. Reichenbach, *Combust. Explos. Shock Waves*, 4 (2) (2010) 271-278.
- [4] A. L. Kuhl, H. Reichenbach, *Proc. Combustion Inst.* 32 (2) (2009) 2291-2298.
- [5] A. L. Kuhl, J. B. Bell, V. E. Beckner, H. Reichenbach, *Proc. Combustion Inst.* 33 (2) (2011) 2177-2185.

- [6] A. L. Kuhl, J. B. Bell, V. E. Beckner, *Combust. Explos. Shock Waves* 46 (4) (2010) 433-448.
- [7] A. L. Kuhl, H. Reichenbach, J. B. Bell, V. E. Beckner, *14<sup>th</sup> Int. Detonation Symp.* ONR-351-10-185 (2010) 806-815.
- [8] A. L. Kuhl, J. B. Bell, V. E. Beckner, K. Balakrishnan, Spherical combustion clouds in explosions, *23<sup>rd</sup> Int. Colloq. Dynamics of Explosions & Reactive Systems* (2011) submitted to SHOCK WAVES.
- [9] A. L. Kuhl, *Khim Fiz (Chem. Phys. RAS)* 25 (10) (2006) 42-48.
- [10] W. M. Howard, A. L. Kuhl, K. S. Vandersall, F. Garcia, D. W. Greenwood, *14<sup>th</sup> Int. Detonation Symp.* ONR-351-10-185 (2010) 81-90.
- [11] *SE-1 Detonator*, Monsanto Research Corporation Report No. MLM-MU-76-70-0008 (1976) 1- 4.
- [12] A. L. Kuhl, R. E. Ferguson, A. K. Oppenheim, T-H J. Sum, H. Reichenbach, P. Neuwald, *Archivum Combustionis* 21 (1) (2001) 3-25.
- [13] H. L. Brode, Rand Corp. Report RM-1965 (1957) 1-61.
- [14] G. N. Nurik, J. B. Martin, *Int. J. Impact Engineering* 8 (2) (1989), 159-186.
- [15] L. I. Sedov, *Similarity and Dimensional Methods in Mechanics*, Academic Press (1959) 1-363.

**WORD COUNT = 2,706 words**

**FIGURE CAPTIONS**

- Fig. 1. Photograph of the barometric calorimeter.  
 Fig. 2. Photographs of the charge assembly and mounting in the calorimeter.  
 Fig. 3. Pressure histories of the reflected blast wave from a C4 charge detonated in air and N<sub>2</sub> (station 1 at GR = 0).  
 Fig. 4. Pressure histories of the reflected blast wave from a C4 charge detonated in air and N<sub>2</sub> (stations 2 and 3 at GR = 5 cm).  
 Fig. 5. Pressure histories of the reflected blast wave from a C4 charge detonated in air and N<sub>2</sub> (station 5 at GR = 10 cm).  
 Fig. 6. Pressure histories of the reflected blast wave from a C4 charge detonated in air and N<sub>2</sub> (station 6 at GR = 15 cm).  
 Fig. 7. Pressure histories of the reflected blast wave from a C4 charge detonated in air and N<sub>2</sub> (station 4 at GR = 20 cm).  
 Fig. 8. Pressure histories of the reflected blast wave from a C4 charge detonated in air and N<sub>2</sub> (station 8 at GR = 25 cm).  
 Fig. 9. Pressure histories of the reflected blast wave from a C4 charge detonated in air and N<sub>2</sub> (station 7 at GR = 30.5 cm).  
 Fig. 10. Positive-phase impulse of the reflected blast wave from a C4 charge detonated in air and N<sub>2</sub> ( $HOB/r_0 = 0.1963$ . Fit 1:  $0.924 - 3.7 * GR/r_0$  and fit 2:  $0.859 - 3.7 * GR/r_0$ )  
 Figure 11. Positive-phase impulse versus ground range for a C4 charge detonated in N<sub>2</sub> compared with an ALE3D code simulation.  
 Figure 12. Peak shock pressure versus ground range for C4 explosion in N<sub>2</sub>: test #2 versus ALE3D simulation (fit:  $168 - 750 * GR/r_0$ ).  
 Fig. 13. Le Chatelier diagram for C4 detonation products (*F*) and combustion products (*CP*).  
 Fig. 14. Cross-section of the temperature field in a turbulent TNT combustion cloud [8]; red indicates  $T = 2,900$  K.  
 Fig. 15. Evolution of the C4 mass-fraction consumed by combustion with air (curve fit:  $81.1 * [1 - 1.55e^{-14.8*t/t_0}]$ ).  
 Fig. 16. Non-dimensional free air curve for C4 (curve fit:  $-5.5 + 1.31 * (r/r_0)^{-1.622}$ ).  
 Fig. 17. Scaled positive phase impulse at  $GR=0$  versus scaled HOB for C4, from ALE3D code simulations (curve fit:  $110 * (HOB/r_0)^{-2.33}$ ).

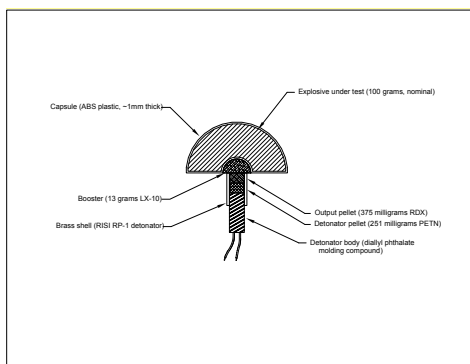
Table 1. Impulse-history fits and chamber pressures

Test	$I(t) = a + \Delta p_c \cdot t$	$p_c (bars)_{measured}$	$p_c (bars)_{predicted}$
#1 (air)	$-7.7 + 8.6378 * t$	9.64	8.21
#3 (air)	$-7.2 + 9.458 * t$	10.46	8.21
#5 (air)	$-6.8 + 8.8506 * t$	9.85	8.21
#2 (N <sub>2</sub> )	$0.062 + 2.9958 * t$	4.00	4.18
#4 (N <sub>2</sub> )	$2.2 + 3.1949 * t$	4.19	4.18
#6 (N <sub>2</sub> )	$1.2 + 3.3141 * t$	4.31	4.18



Fig. 1. Photograph of the barometric calorimeter

(a) charge schematic



(b) charge assembly



(c) assembly installed in calorimeter



Fig. 2. Photographs of the charge assembly and mounting in the calorimeter.

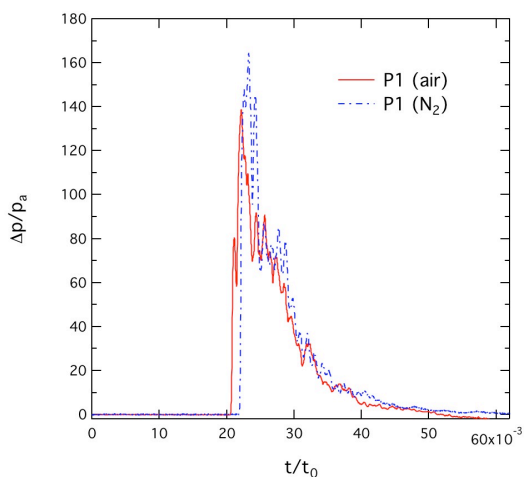


Fig. 3. Pressure histories of the reflected blast wave from a C4 charge detonated in air and N<sub>2</sub> (station 1 at GR = 0).

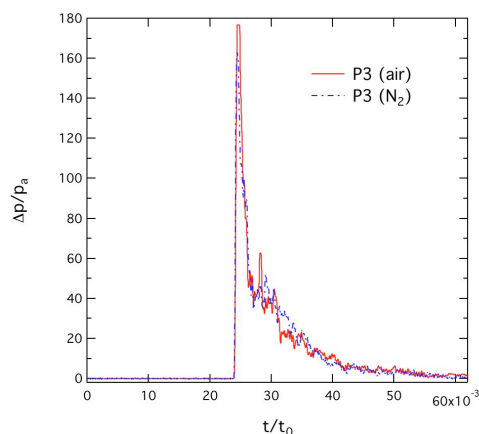
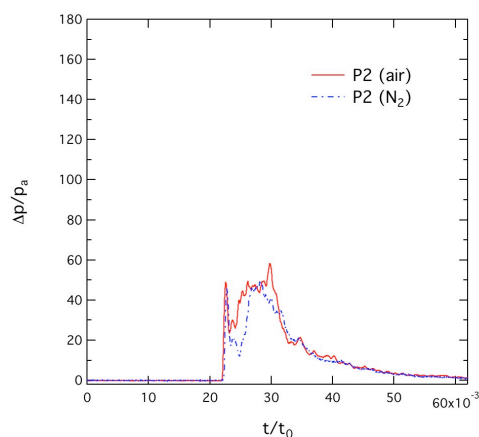


Fig. 4 Pressure histories of the reflected blast wave from a C4 charge detonated in air and N<sub>2</sub> (stations 2 and 3 at GR = 5 cm).

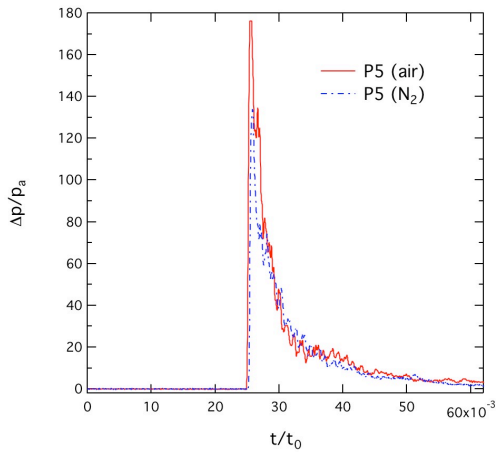


Fig. 5. Pressure histories of the reflected blast wave from a C4 charge detonated in air and N<sub>2</sub> (station 5 at GR = 10 cm).

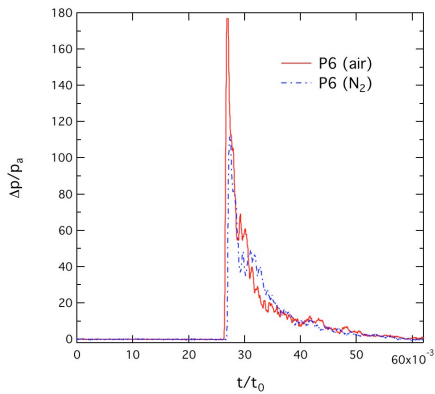


Fig. 6. Pressure histories of the reflected blast wave from a C4 charge detonated in air and N<sub>2</sub> (station 6 at GR = 15 cm).

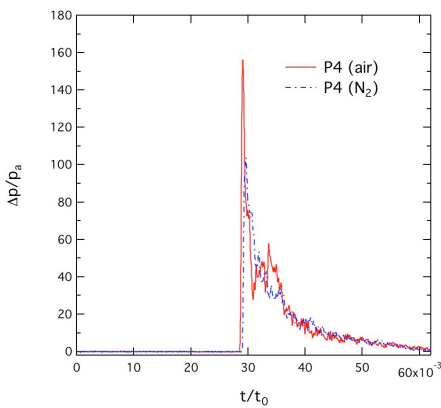


Fig. 7. Pressure histories of the reflected blast wave from a C4 charge detonated in air and N<sub>2</sub> (station 4 at GR = 20 cm).

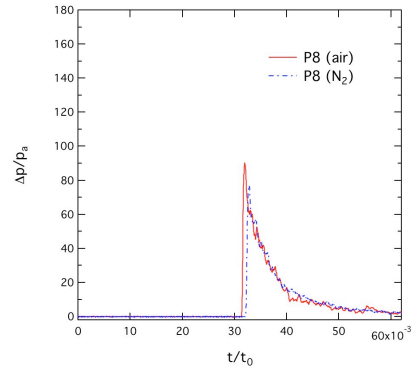


Fig. 8. Pressure histories of the reflected blast wave from a C4 charge detonated in air and N<sub>2</sub> (station 8 at GR = 25 cm).

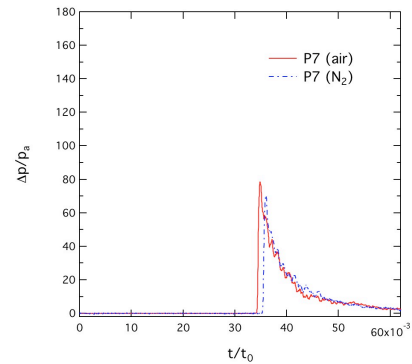


Fig. 9. Pressure histories of the reflected blast wave from a C4 charge detonated in air and N<sub>2</sub> (station 7 at GR = 30.5 cm).

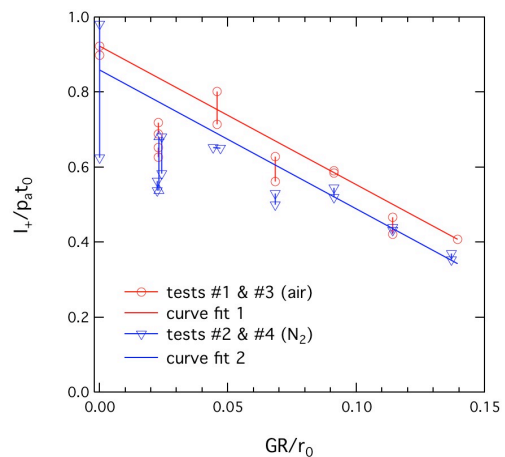


Fig. 10. Positive-phase impulse of the reflected blast wave from a C4 charge detonated in air and N<sub>2</sub>  $HOB/r_0 = 0.1963$ . Fit 1:  $0.924 - 3.7 * GR/r_0$  and fit 2:  $0.859 - 3.7 * GR/r_0$

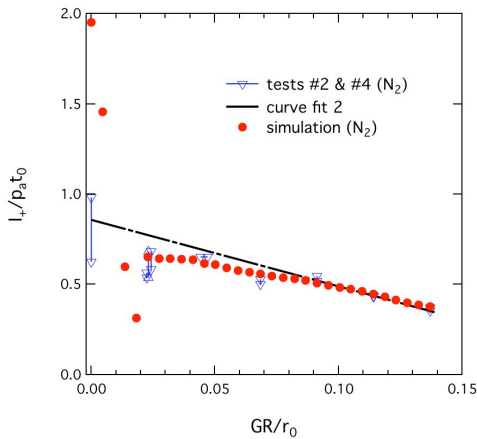


Figure 11. Positive-phase impulse versus ground range for a C4 charge detonated in  $N_2$  compared with an ALE3D code simulation.

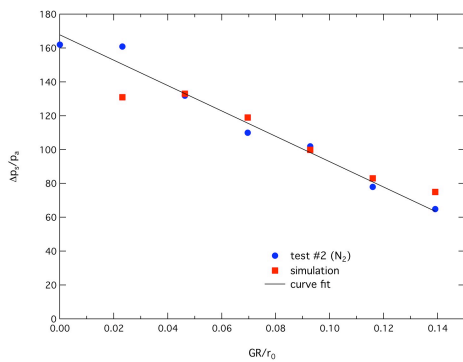


Figure 12. Peak shock pressure versus ground range for C4 explosion in  $N_2$ : test #2 versus ALE3D simulation (fit:  $168 - 750 * GR / r_0$ ).

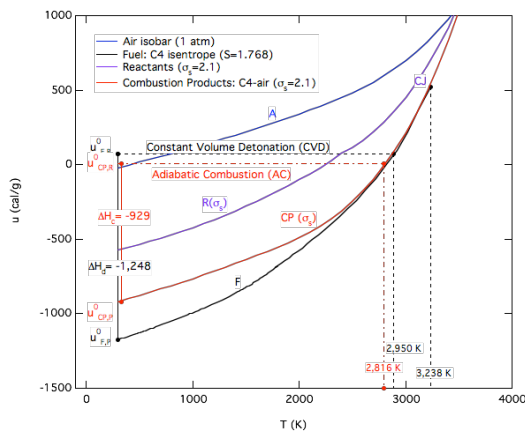


Figure 13. Le Chatelier diagram for C4 detonation products ( $F$ ) and combustion products ( $CP$ ).

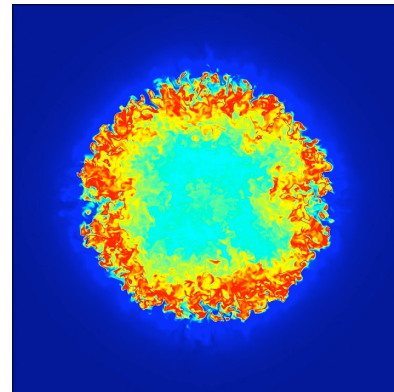


Fig. 14. Cross-section of the temperature field in a turbulent TNT combustion cloud [8]; red indicates  $T = 2,900$  K.

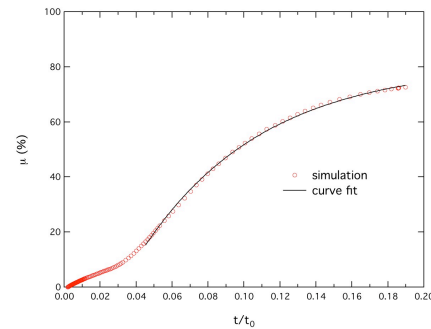


Figure 15. Evolution of the C4 mass-fraction consumed by combustion with air (curve fit:  $81.1 * [1 - 1.55e^{-14.8 * t/t_0}]$ ).

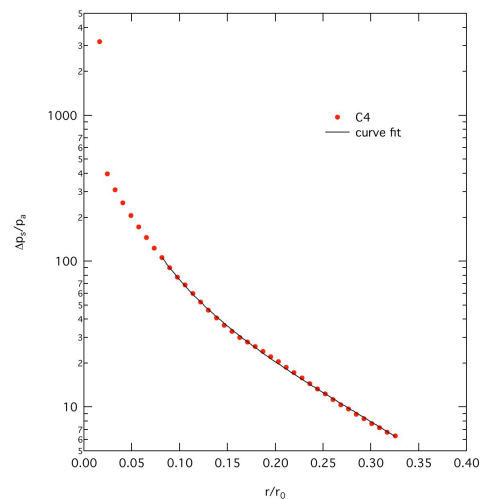


Figure 16. Non-dimensional free air curve for C4 (curve fit:  $-5.5 + 1.31 * (r / r_0)^{-1.622}$ ).

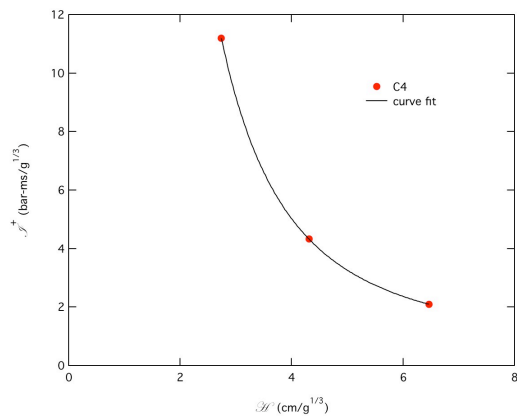


Fig. 17. Scaled positive phase impulse at  $GR=0$  versus scaled HOB for C4, from ALE3D code simulations (curve fit:  $110 * (HOB / r_0)^{-2.33}$ ).

**COUNT:**

3.2 pages of figures \* 900 = 2,880 words

text = 2,706

fig = +2,880

**total = 5,586 words (6,200 limit)**